

Supporting Information

One-step Route for the Conversion of Cd waste to CdS quantum dots by *Acidithiobacillus* sp. via Special Biosynthesis Pathways

Xiao-Ju Li^{a*}, Tian-Qi Wang^a, Lu Qi^b, Feng-Wei Li^a, Yong-Zhen Xia^a, Bin-Jin^c, Cheng-Jia Zhang^a, Lin-Xu Chen^{a*}, and Jian-Qun Lin^{a*}

The sequence of the OSH enzyme in *A. ferrooxidans*, the OSH enzyme in *A. caldus* studied in this work, and the homologous proteins of cystathionine gamma-synthase were used for comparison:

cystathionine gamma-synthase [*Stenotrophomonas maltophilia*]

NCBI Reference Sequence: WP_012509966.1

```
MSNATSQDRALALATLAIHGGQSPDPSTGAVMPPIYATSTYAQSSPGEHQGFYRSRTHNPTRFAYERCVASLEGG  
TRGFAFASGMAASSTVIELLDAGSHVVAMDDIYGGSFRLFERVRRRTAGLDFSFVDLTDLAAFEASITPKTKM/VW  
IETPTNPMLKIVDIAAVAAIAKRHGLIVVDNTFASPMLQRPLELGADLVLSATKYLNGHSDMVGGMVVVDNA  
ELAEQMAFLQNSVGGVQGPFDLALRGLKTLPLRMKAHCANALALAQWLEKHPAVEKVIYPGLASHPQHELAKG  
QMAGYGGIVSIVLKGGFDAAKRFCEKTELFTLAESLGGVESLVNHPAVMTHASIPVARREQLGISDALVRLSVGV  
EDLGDLQVDLGEALK
```

O-succinylhomoserine sulfhydrylase [*Acidithiobacillus ferrooxidans*]

NCBI Reference Sequence: WP_012536942.1

```
MNTKNTNPDWADRLRPETIAIRAGIHRTOEQEHSEAIFFPTSSVFVDSAEAAADRFAGRVPGNIYARFTNPTVVRTF  
EERLAALEGAEACVATASGMAACLTA FMGILKAGDHVVASRSIFGTTVQLLGNILSRFGVETS FVPLADVPAWRA  
ALRPNTRMLFLETPSNPLTEIGDMQALADLAHVHDVLDVVDNCFCTPALQQPLKFGADLVIHSATKYLDGQGRTL  
GGAVCGSTELLNSGPRNFVRTAGPSLSPFNWVQLKGLETLGLRMRHCANAQKIAEWLEARPEVARVYYPGLDS  
HPQQALAAARQQRLPGAILSFDLHGGQKAAWAFVDALRLLSLTANLGDAKTTITHPASTTHSRVSPPEARAAAGVGD  
GLLRISVGLEHADDLREDMERGFALVAR
```

O-succinylhomoserine sulfhydrylase [*Acidithiobacillus caldus* MTH-04]

NCBI Reference Sequence: WP_004873154.1

```
MTEKSEPHGKWRPETLAIRAGVHRSAEKEHAEALFLTSSVFVDSAEAAAARFAGTSPGNIYARFTNPTVRALEER  
LAALEGAEDCVATASGMAACLTTFMGLLQAGDHIVASRSIFGSTIQLLQNILGRFGLETTFFVALDDLAAWRRALR  
PNTRLLYLETSPNPLTEIGDISALAAAREHGASLVVDNCFCTPVLLQQLALGADLVIHSNTKYLDGQGRTLGGA  
ICGRKELLAGPRNFVRTAGPSLSPFNWVQLKGLETLALRMRHSHNALELARWLEQREEVARVYFPGLASHPQQ  
VLAERQQRLPGGILSFDLHGGQAAAWALMNAVEIFSRTANLGDAKSTITHPASTTHGRVSAEAAAAGIGDGLLR  
LSVGLEHVDDLRADLARGLEAAATAAASSGA*
```



Figure S1: SDS-PAGE gel of cell lysate (lane 1) and purified OSH enzyme (lane 2) of *Acidithiobacillus caldus* MTH-04 showing a size of about 42 kDa.

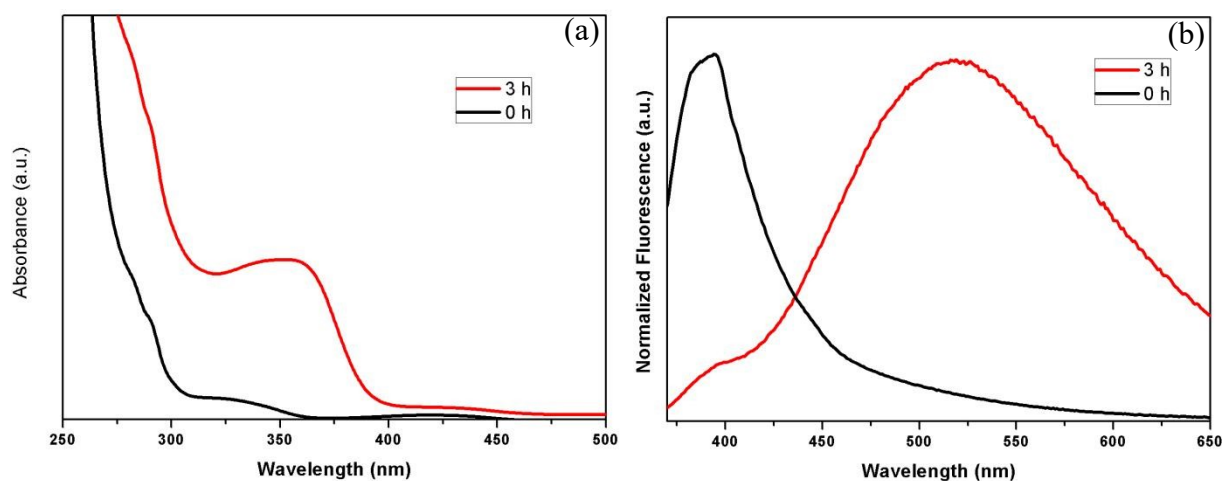


Figure S2: Optical properties of CdS versus synthesis time by the OSH enzyme of *Acidithiobacillus ferrooxidans* ATCC23270: (a) Photographs of photoluminescence under UV light at various time intervals. (b) Absorbance spectra of OSH (1 mg/mL) incubated with 5 mM cysteine and 0.5 mM cadmium acetate for different time intervals.

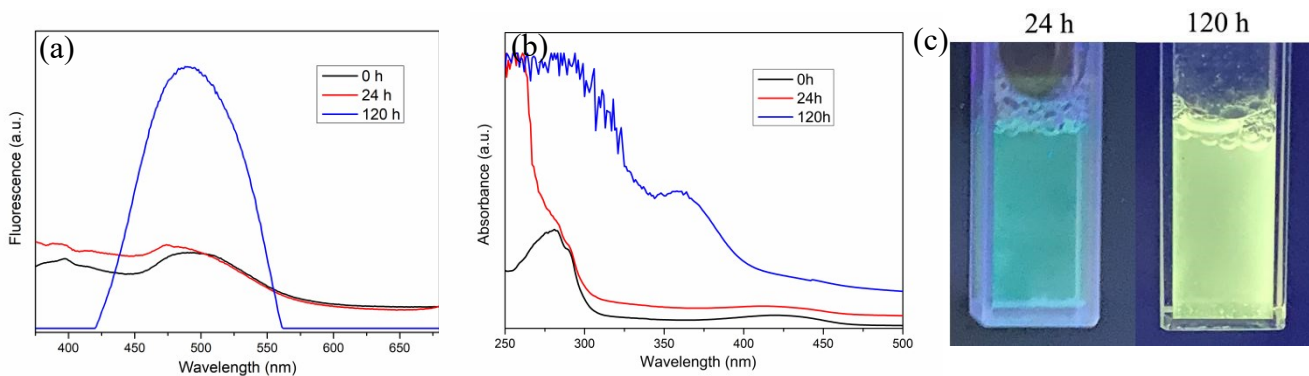


Figure S3: Optical properties of CdS versus synthesis time by the OSH enzyme of *Acidithiobacillus caldus* MTH-04: (a) Photographs of photoluminescence under UV light at various time intervals. (b) Absorbance spectra of OSH (1 mg/mL) incubated with 5 mM GSH and 0.5 mM cadmium acetate for different time intervals. (c) Corresponding fluorescence spectra at selected time intervals using an excitation wavelength of 350 nm.

Table 1

Data collection and refinement statistics (molecular replacement)

Wavelength	1.542
Resolution range	22.87 - 2.27 (2.351 - 2.27)
Space group	C 1 2 1
Unit cell	130.768, 82.7873, 77.49, 90, 110.313, 90
Total reflections	123255 (3704)
Unique reflections	34171 (2285)
Multiplicity	3.6 (1.6)
Completeness (%)	95.10 (69.00)
Mean I/sigma (I)	17.80 (5.10)
Wilson B-factor	22.76
R-merge	0.046 (0.125)
R-meas	0.051 (0.156)
R-pim	0.026 (0.111)
CC1/2	0.998 (0.967)
Reflections used in refinement	34093 (2487)
Reflections used for R-free	1734 (124)
R-work	0.1623 (0.1953)
R-free	0.2148 (0.2835)
Number of non-hydrogen atoms	6567
macromolecules	6048
ligands	30
solvent	489
Protein residues	789
RMS(bonds)	0.004
RMS(angles)	0.67
Ramachandran favored (%)	98.09
Ramachandran allowed (%)	1.91
Ramachandran outliers (%)	0.0
Rotamer outliers (%)	2.26
Clashscore	2.57
Average B-factor	26.44
macromolecules	26.22
ligands	21.65
solvent	29.45

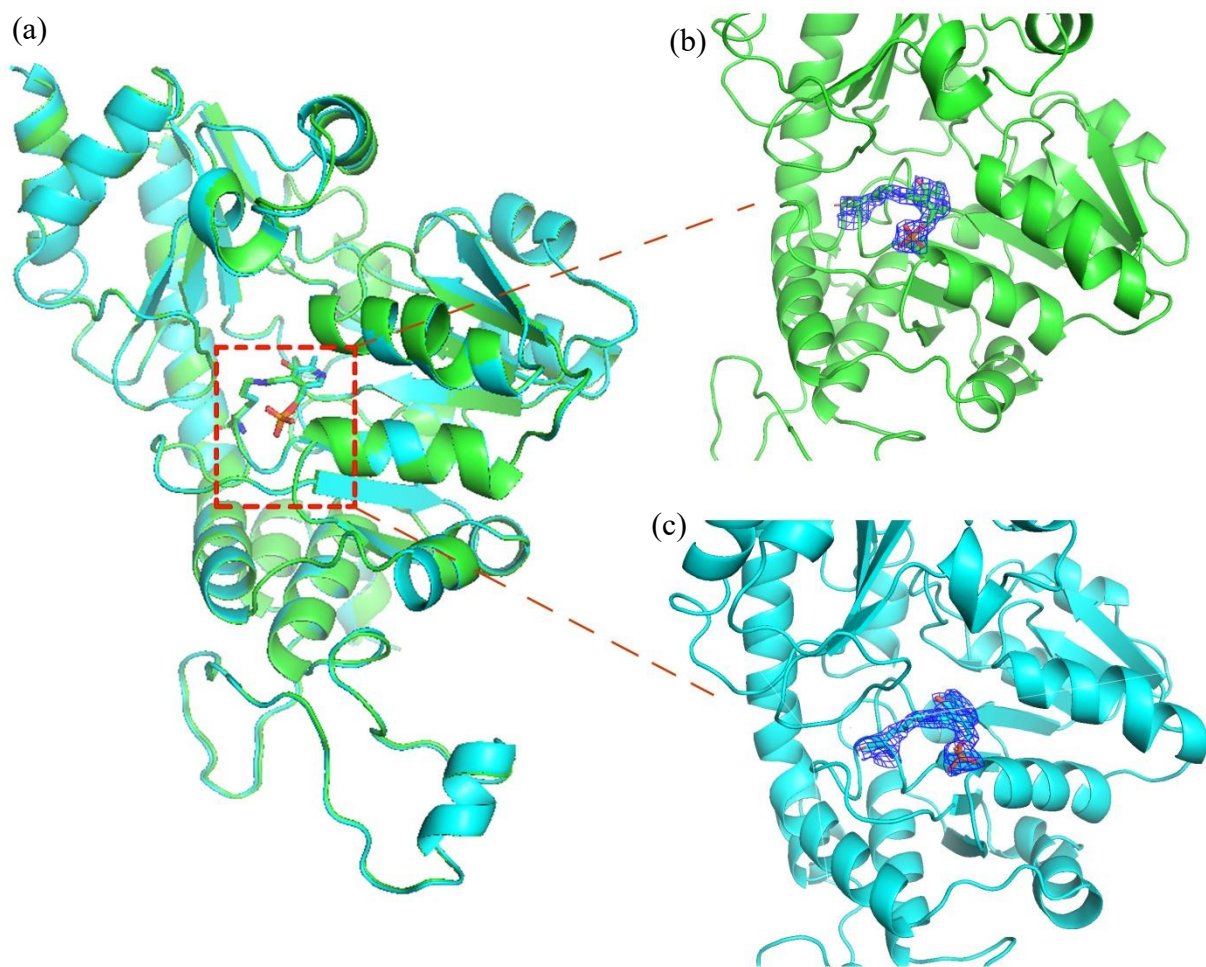


Figure S4: (a) A and B monomers of the OSH structure are aligned together, showing that the individual monomers are very similar. (b) and (c). The PLP exists in the A and B monomers.

There are two *sqr* genes in *A.caldus* MTH-04: *orf1436* and *orf2678*. The corresponding *SQR* (Sulfide quinone reductase) enzymes were studied in this work, and their sequences are as follows:

SQR1 enzyme (*orf1436*)

MSNKPHVVVLGGNFAGLGAAQKIREFAGDAVRITVIDRKNFLLFVFNIPAEVFEGRDPAKTLMSDLRSTLAEDDI
GFIQAEVQALDPAKRIDFVPSERPGAAPESMHYDYVVAVGNRLAFDRIEGFAEHGHTCTDFYYGNKLRHFLEH
EYRGGPVAIGSARFHQGDGTDIKLYGGHAFPSAEAAACEGPPVETMLSMATWLKEHGKGGPDKITVFTPAKLIAE
DAGEQVVGKLEIASGMGFHYLNETQDITRITHEGVEFANGKSVEAELKLVFPDWPVPHDFLKGLPISDSEGFVVT
DVTMRNPKYPNVFAAGDAAAITVPKLGGIGHAEGEIVGKQIAKDVGRMAAEEADKPLEPVVYICIGDMGANQAFYI
RSNSWFGGPDQVLKMGHVPFLLKMQYKNLFFKTRGKMPWGLDASKLLAEKLFAA*

SQR2 enzyme(*orf2678*)

MAHVILGAGTGGMPAAYEMKDALGKDHEVTLISANDYFQFVPSNPWLGVGWSKREDITFPPIRPHYVERKGIHFIP
QRAEKIDAQKQEIQLADGSSVHYDYLLIATGPKLAFENVPGSDPHEGVPVQSVCTADHAEMAYGKYQELLDNPGPI
VIGAMPGASCFGPAYEYAMIVASDLKKRGMRDKIPSFVFTSEPYIGHLGIQGVGDSRGILTRGLEEEGITAYTN
CKVTKVENGQMYITQVNDQGETVKEFTLPVKFGMMIPAFKGVPAVAGVEGLCNPGGFVLVDENQRSKYPNIYAA
GIAIAIPPEQTPVPTGAPKTGYMIESMVSAAVHNIKADIEGRKGERTMGTWNAVCFADMGDRGAAFVALPQLKP
RKVDVFAYGRWVHLAKVAFEKYFIRKMKMGVSEPFYEKVLFKMMGITRLKEEPMEQRKAS*

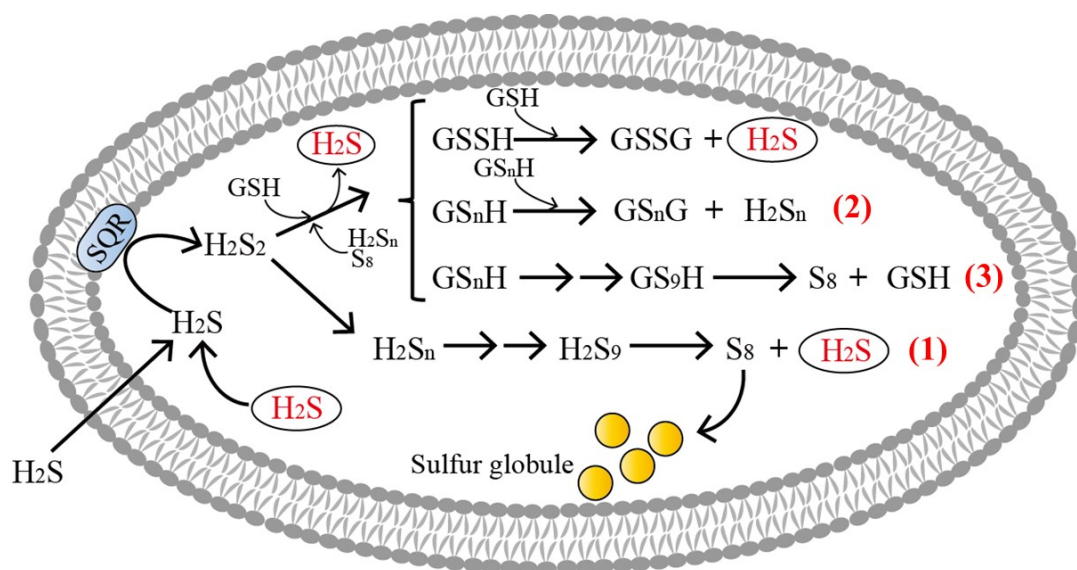


Figure S5. The proposed process of converting H_2S to Sulfur globules (S_8) in SQR bacteria.

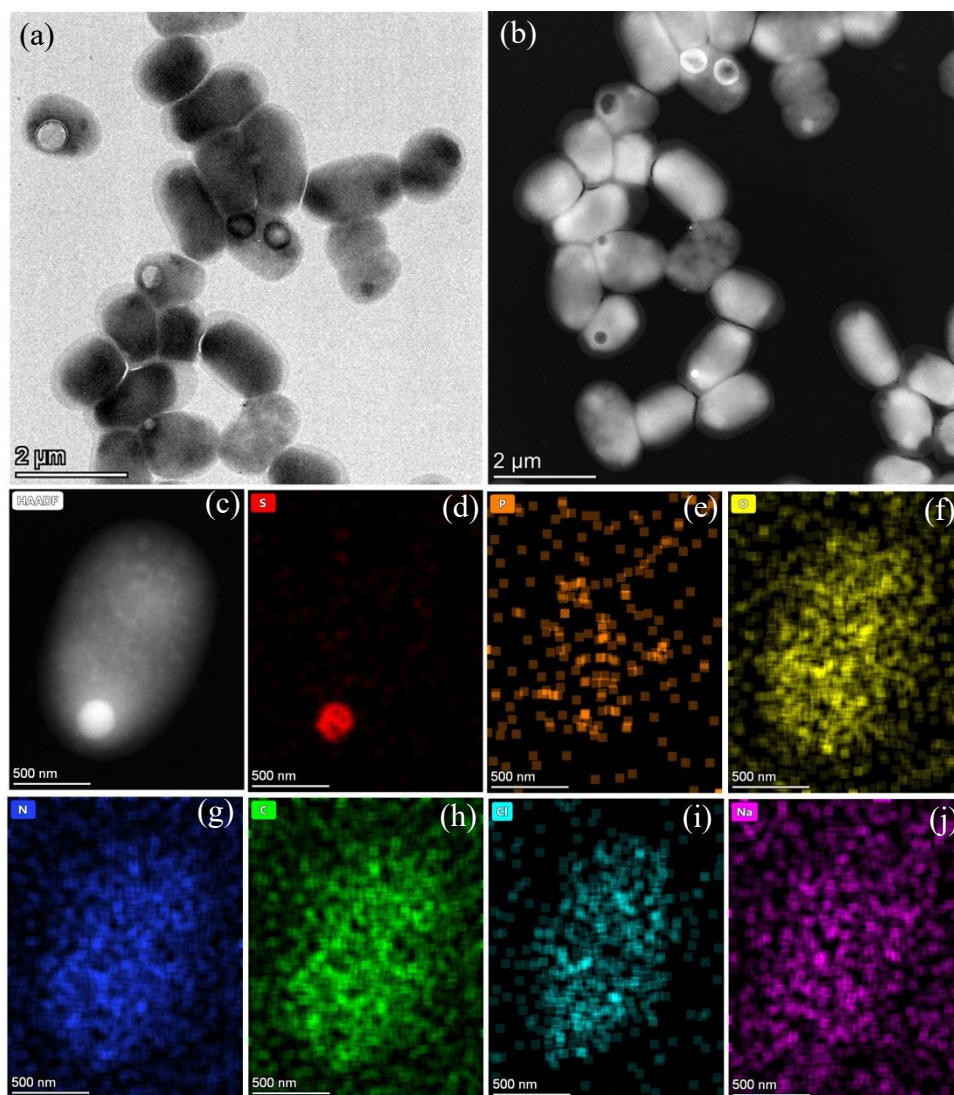


Figure S6. Sulfur globules accumulated in *Escherichia coli*, in which heterologously overexpress SQR1. (a) Transmission electron microscopy and (b) Scanning transmission electron microscopy images of unstained *Escherichia coli*. (c) One bacterium image and its corresponding (d-j) elemental maps of sulfur, phosphorus, oxygen, nitrogen, carbon, chlorine and sodium by energy-dispersive X-ray spectrometry.

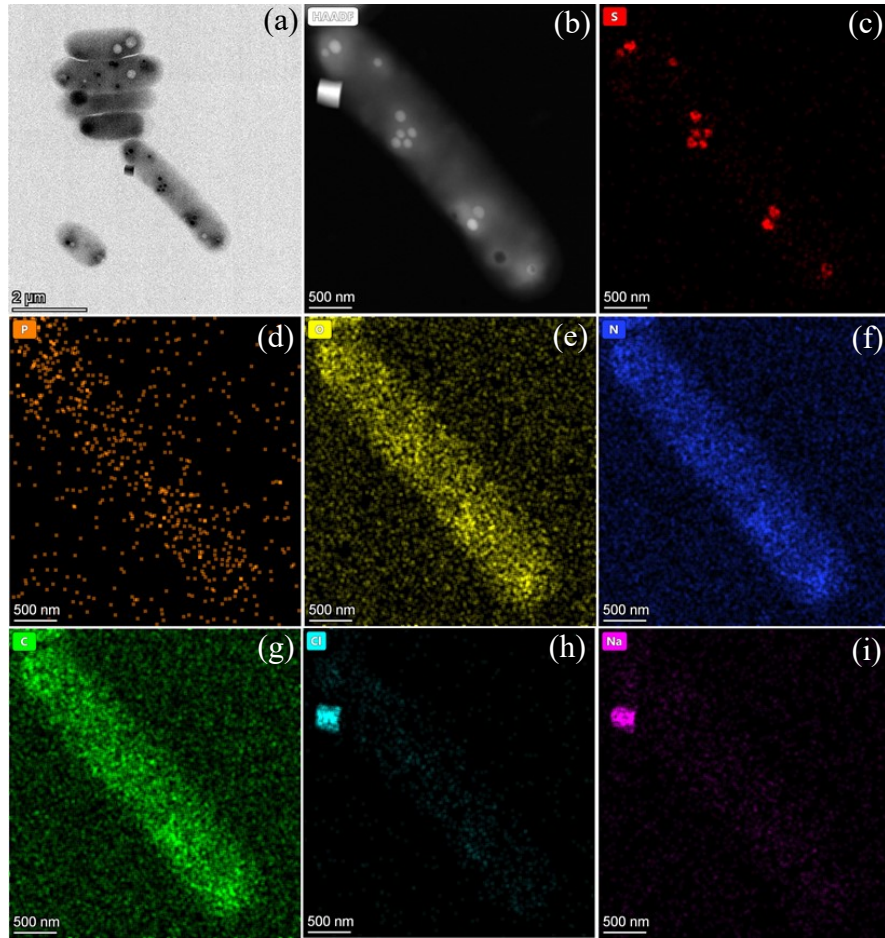


Figure S7. Sulfur globules accumulated in *Escherichia coli*, in which heterologously overexpress SQR2. (a) Transmission electron microscopy, and (b) Scanning transmission electron microscopy images of unstained *Escherichia coli*. (c-i) The corresponding elemental maps (the bacteria in b) of sulfur, phosphorus, oxygen, nitrogen, carbon, chlorine, and sodium by energy-dispersive X-ray spectrometry (EDS).

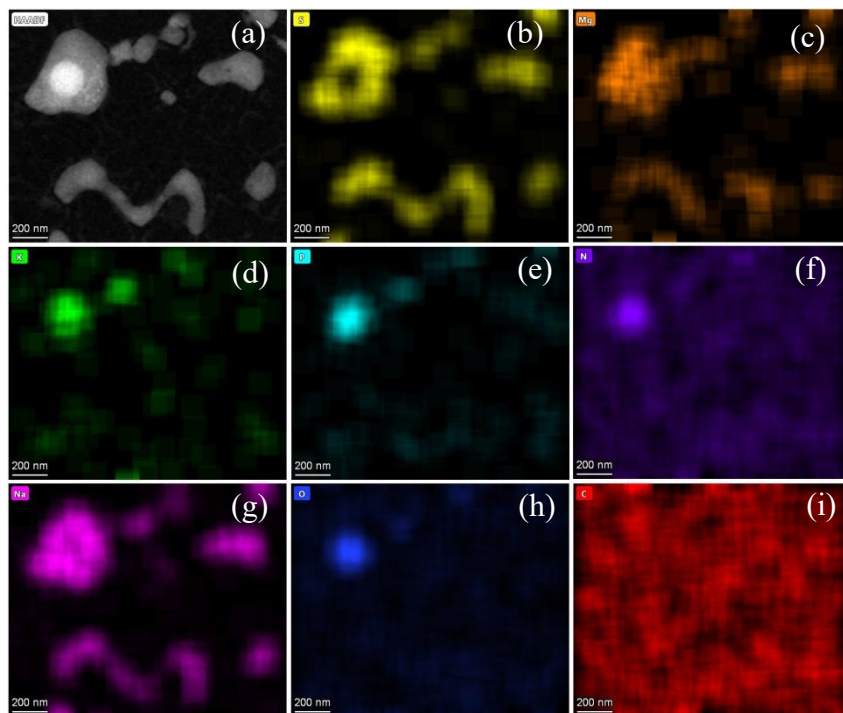


Figure S8. Scanning transmission electron microscopy image (a) and its corresponding elemental maps (b-i) of one extracellularly distributed polyphosphate sphere in *A. caldus* culture, implying that the polyphosphate sphere is covered by some activated sulfur-enriched substance.

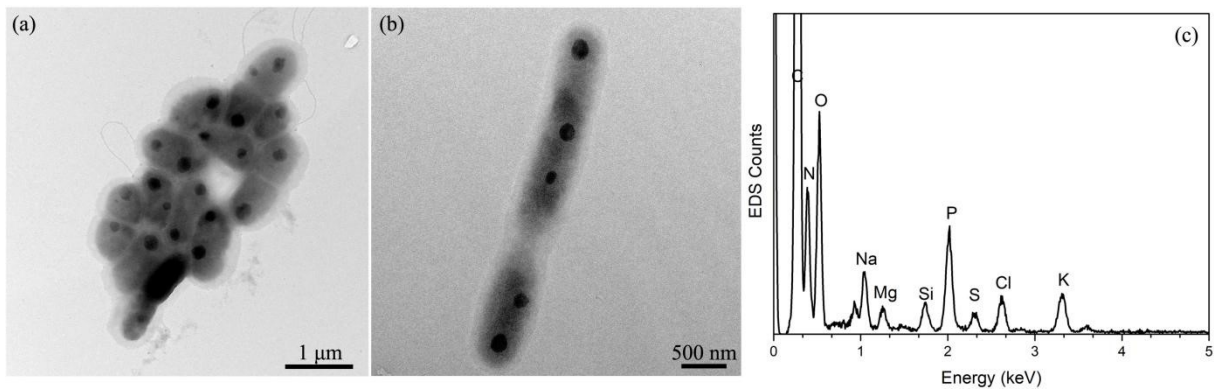


Figure S9. Transmission electron microscopy images of (a) *A. caldus* and (b) *A. ferrooxidans*, (c) EDS composition of one extracellular polyphosphate, showing the polyphosphates observed in the intracellular space in *Acidithiobacillus* sp.

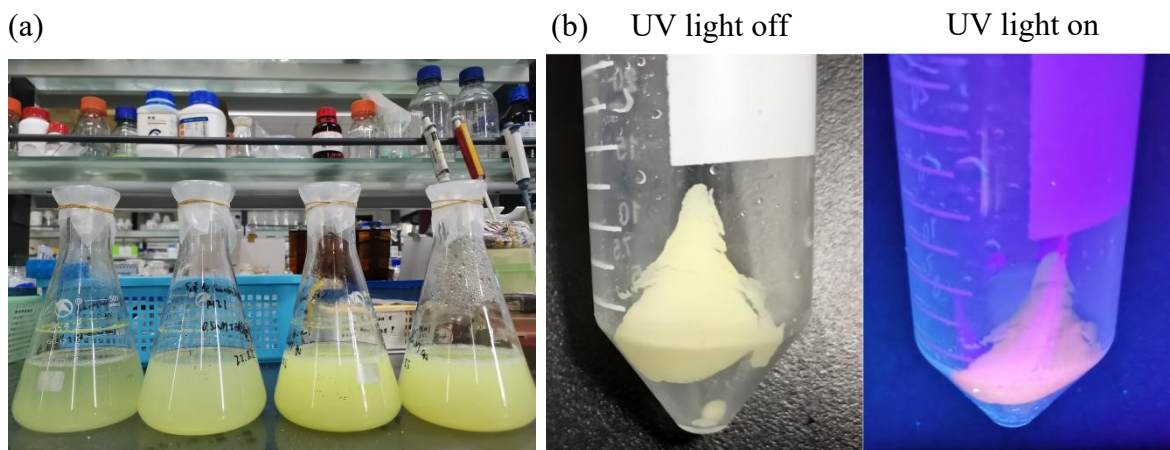


Figure S10. Addition of cysteine and cadmium acetate to the supernatant solution of sulfur cultured *A. caldus* and after 3 days reaction: (a) A photograph of the final products showing a yellow color, indicating that CdS is indeed biosynthesized in this solution. (b) Photograph of the centrifugal precipitation of the final products under illumination with white light (left) and UV (365 nm) light (right). The supernatant solution had no obvious fluorescence, and only the centrifugal precipitation showed pink fluorescence.

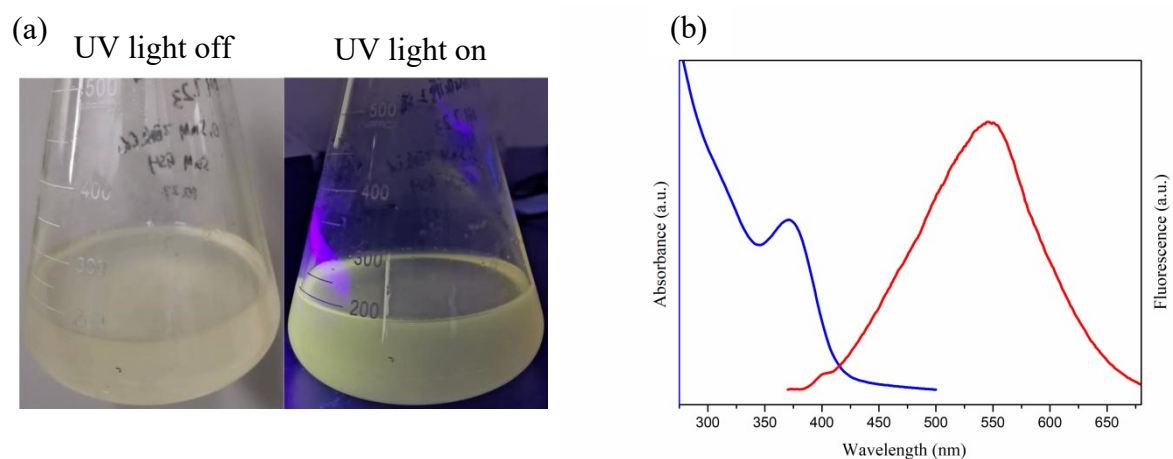


Figure S11. The addition of GSH and cadmium acetate to the supernatant solution of $K_2S_4O_6$ cultured *A. caldus* and after 3 days reaction: (a) Photograph of the supernatant under illumination with white light (left) and UV (365 nm) light (right). Obvious fluorescence in supernatant solution can be observed, implying that the CdS QDs were biosynthesized successfully. (b) Absorbance and corresponding fluorescence spectra of the supernatant at an excitation wavelength of 350 nm.

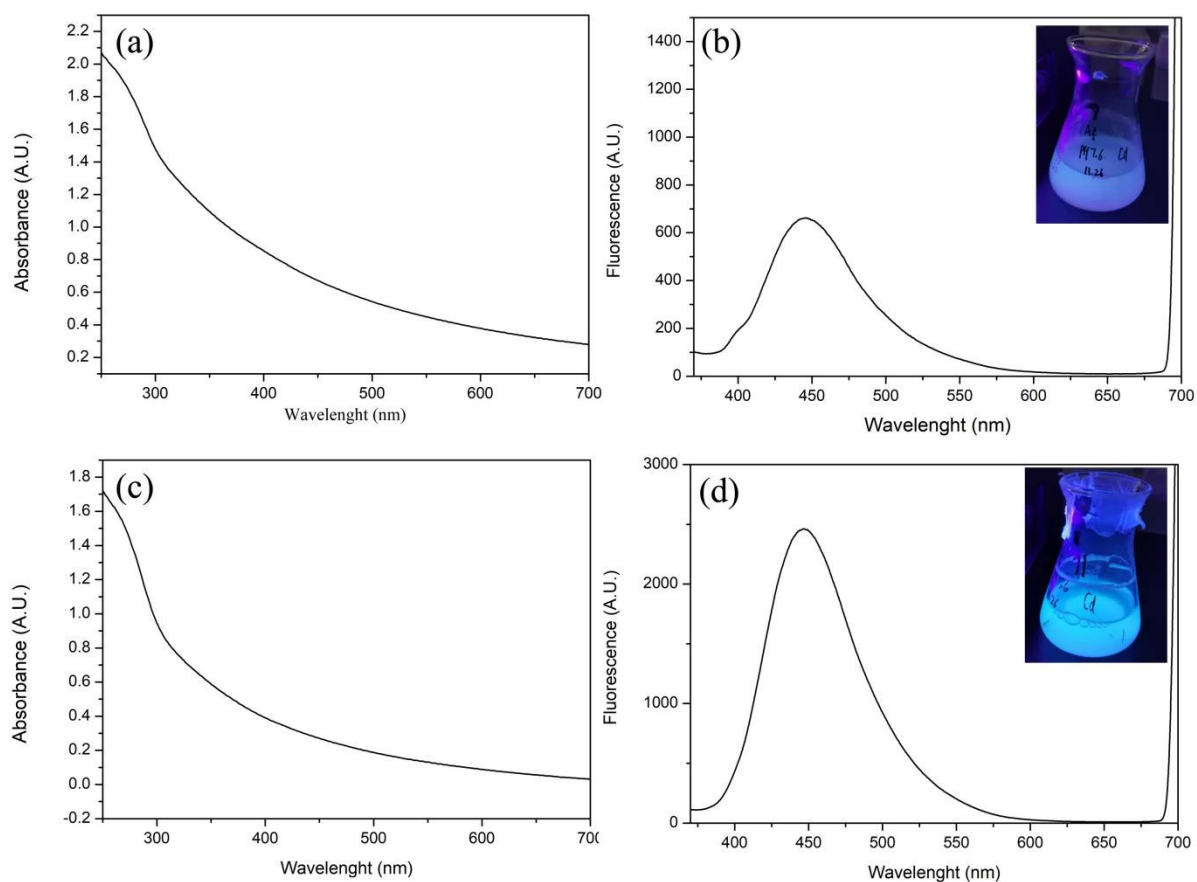


Figure S12. After culturing the *Acidithiobacillus* sp. to the logarithmic growth phase, the culture supernatant pH was adjusted to approximately 7.0 with KOH, and the cells were removed by centrifugation. Both *A. ferrooxidans* (a,b) and *A. caldus* (c,d) show obvious spontaneous blue-green fluorescence.

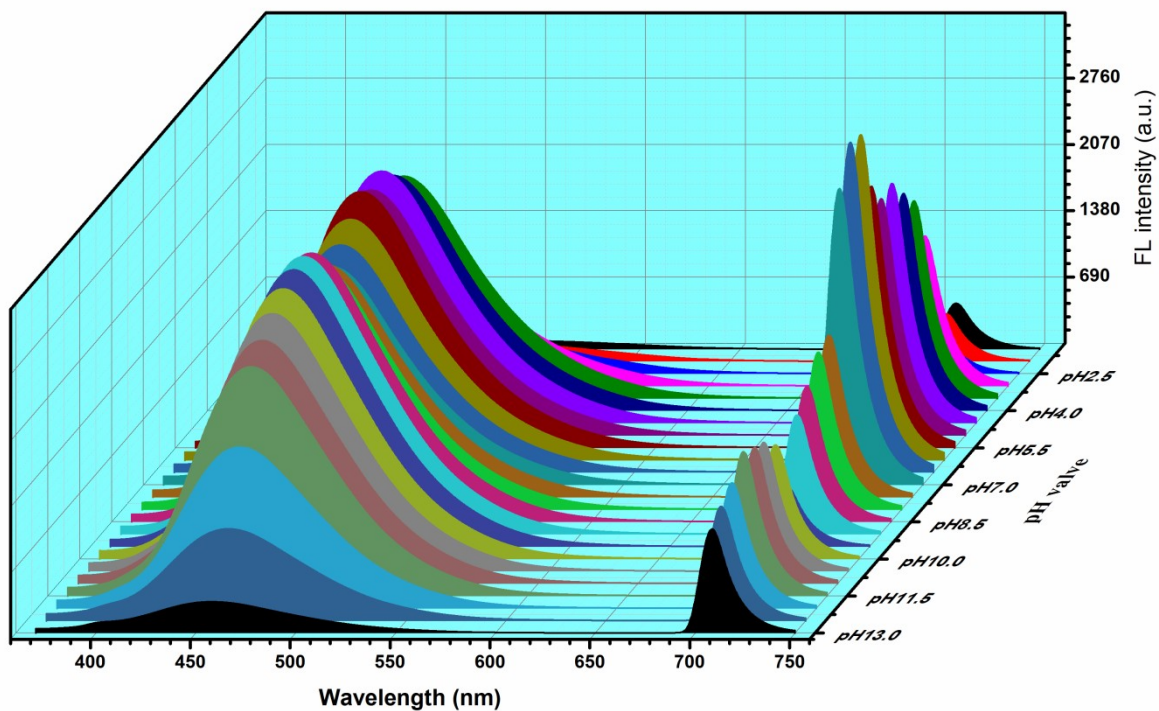


Figure S13. The fluorescence spectra (using an excitation wavelength of 350 nm) of the culture supernatants of *A. caldus* incubated for 7 days and then removal of *A. caldus* cells by centrifugation, with difference pH values ranging from 2.5 to 13.0 were obtained by KOH adjustment, revealing that the appearance of spontaneous fluorescence is inhibited by the acidic environment and that once the pH is adjusted to a relatively mild range, it will spontaneously appear.

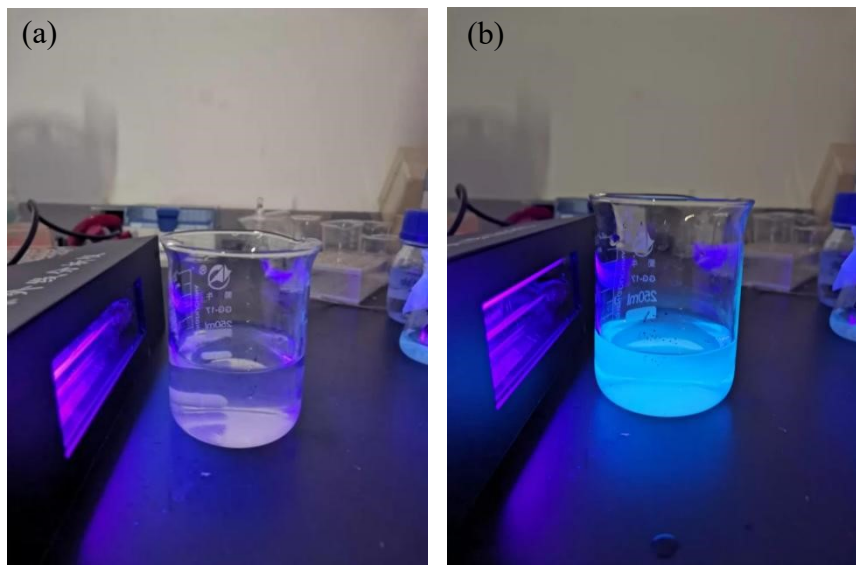


Figure S14. Photoluminescence under UV light (365 nm): (a) Starkey media and (b) culture supernatants of *A. caldus* incubated for 7 days and then after removal of *A. caldus* cells by centrifugation. Both pH values were adjusted to 7 by KOH, while the blue-green fluorescence only appeared in (b), confirming that the spontaneous fluorescence substances were not from the initial media but from the bacterial culture process.

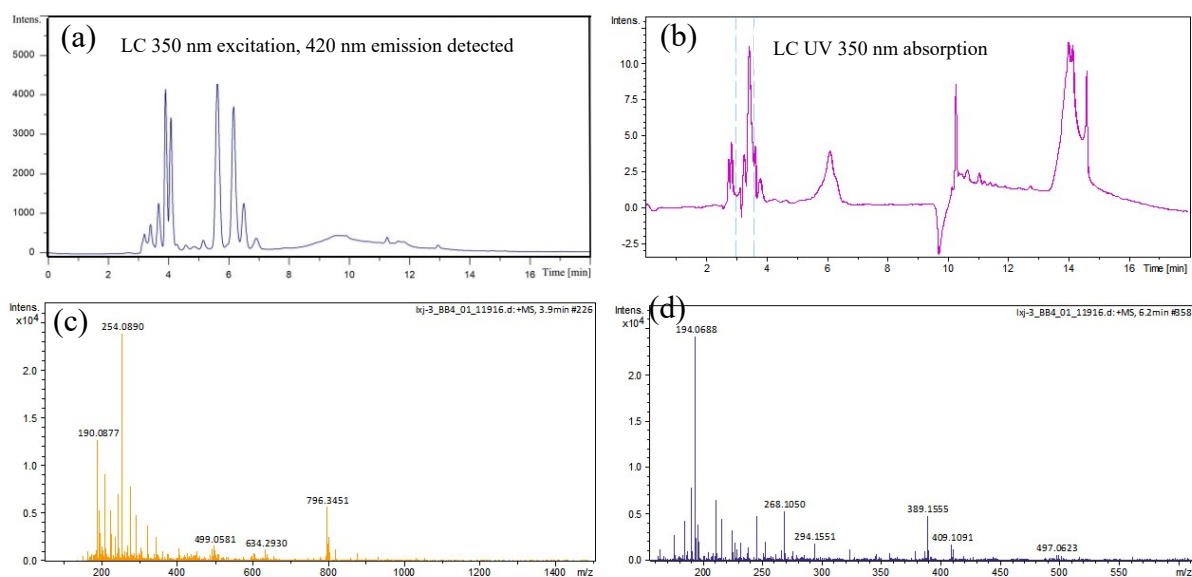


Figure S15. A detailed analysis of the spontaneous fluorescence substances in the culture was conducted. Fermented bacteria (*A. caldus*) were freeze-dried, after which large amounts of inorganic salts were removed by methanol redissolution. The spontaneous fluorescence substances were dissolved in methanol, and then, the mixtures were analyzed by high performance liquid chromatography (HPLC) and liquid chromatography-mass spectrometry (LC-MS) with a C18 analytical column. (a) HPLC spectrum of spontaneous fluorescence substances was obtained using a fluorescence detector with 350 nm excitation and 420 nm detection. (b) HPLC spectrum of spontaneous fluorescence substances with 350 nm absorbed detection. Substance mass analysis of (c) 3.9 min and (d) 6.2 min absorption. These results confirm that the spontaneous fluorescence substances are not inorganic salts, but are organic small molecules with a molecular weight of several hundred.

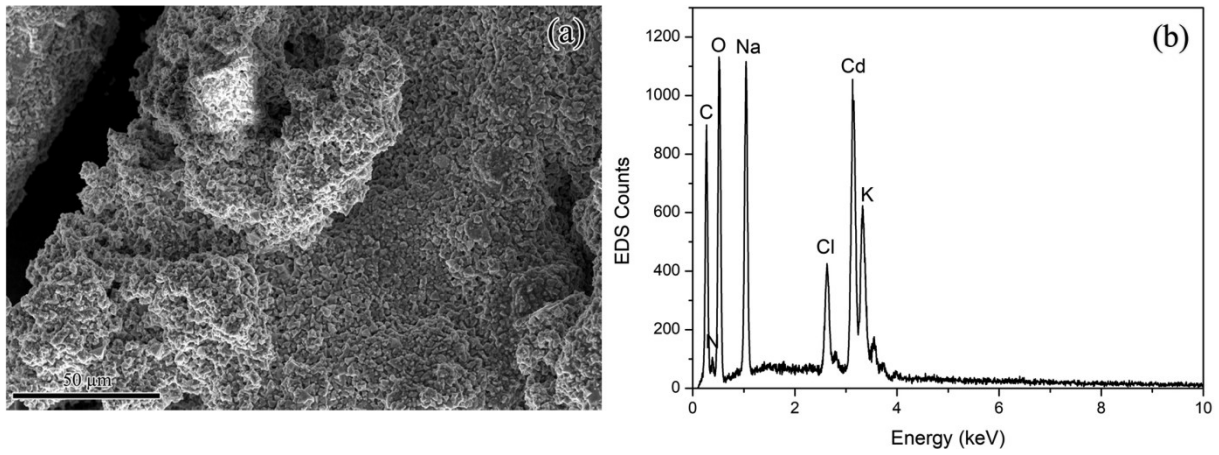
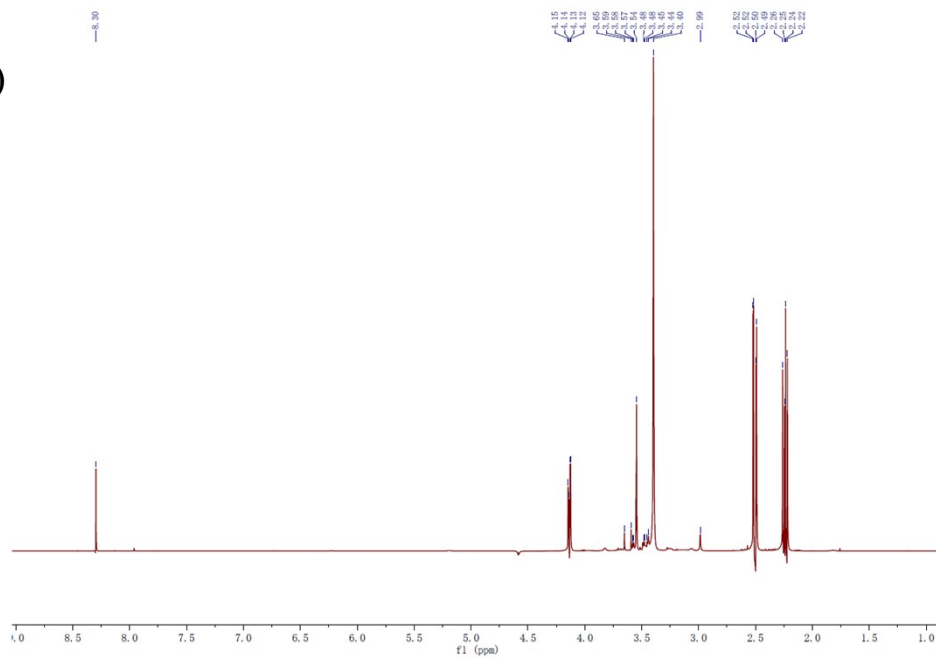
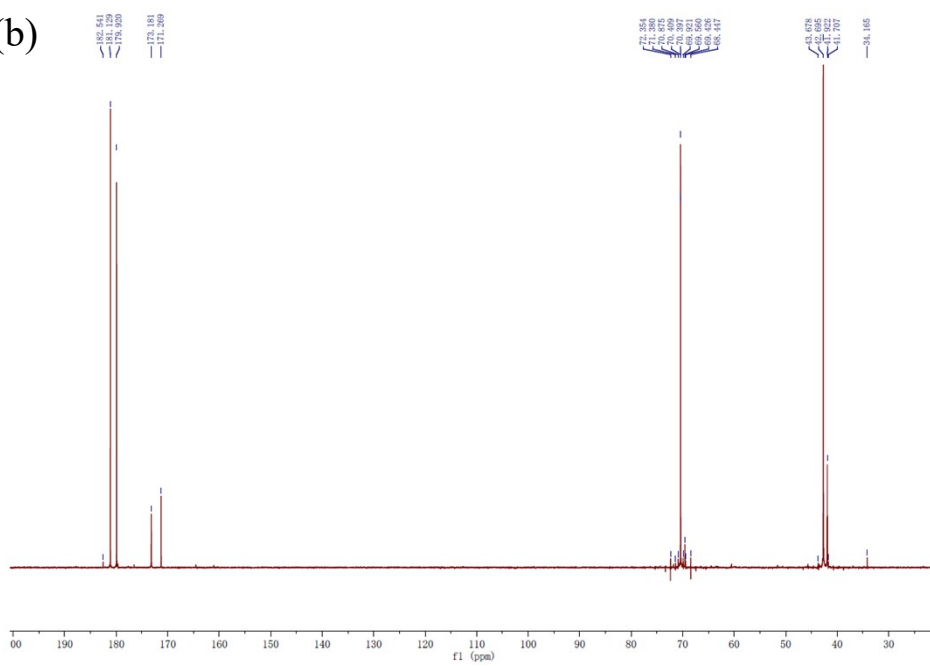


Figure S16. Initial information of cadmium electroplating waste: (a) SEM image and (b) its corresponding composition by EDS. In addition to Cd element, there is a large amount of Na, K, Cl, C and O.

(a)



(b)



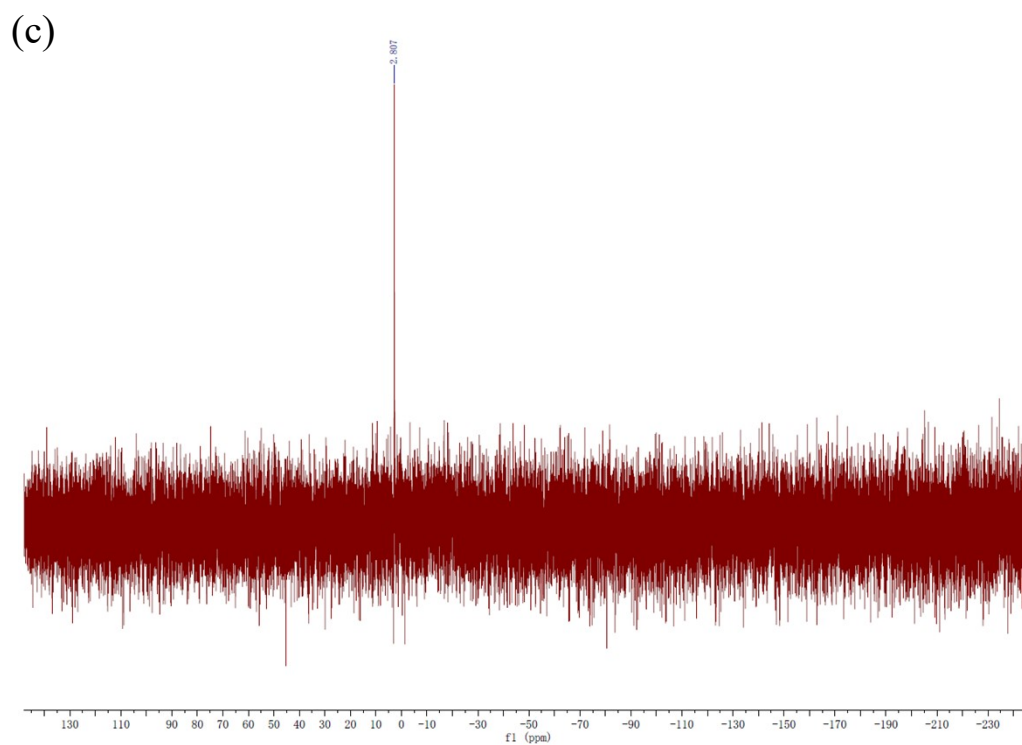


Figure S17. The initial cadmium electroplating waste has trace water solubility, and the NMR data of (a) ^1H , (b) ^{13}C , and (c) ^{31}P can also be obtained using these small amounts of sample in water. These results imply that cadmium electroplating waste is not a simple cadmium precipitation but a complex precipitation that contains large amounts of organic matter and cadmium.

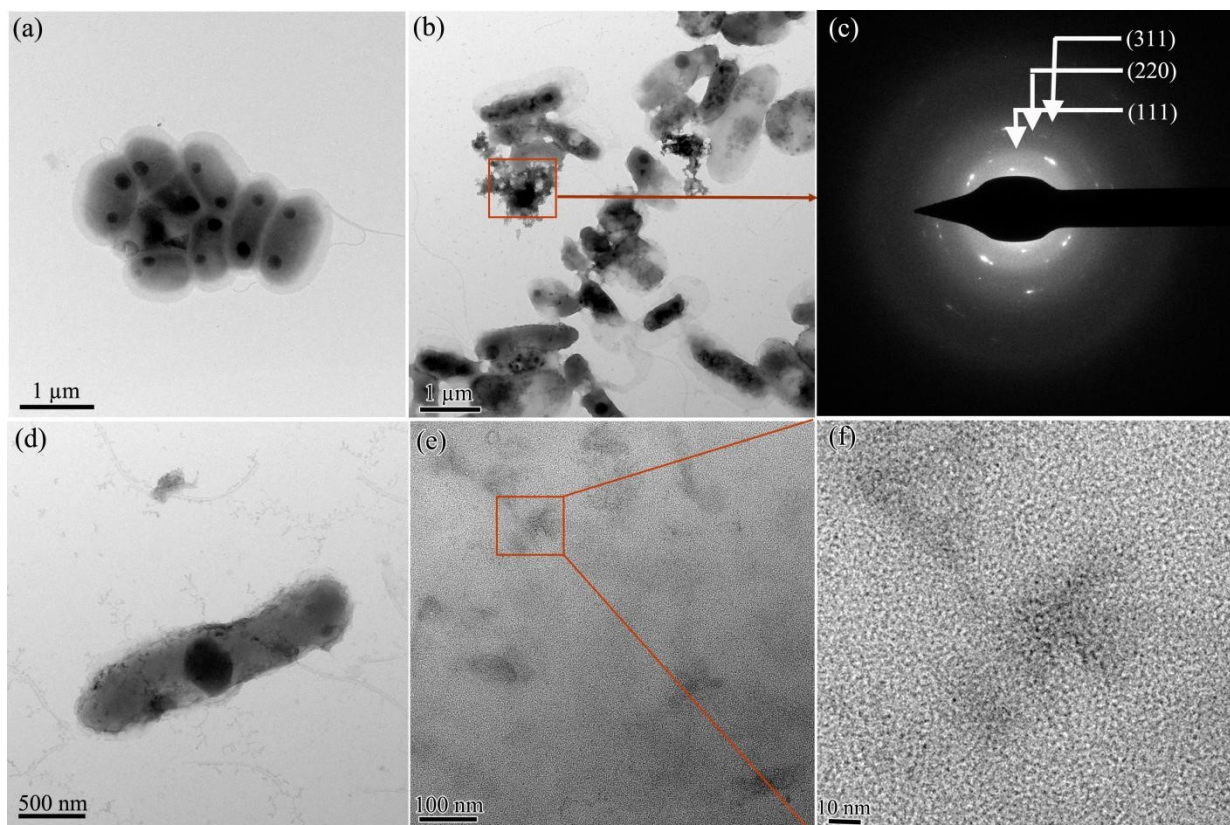


Figure S18. Some CdS QDs precipitated at the extracellular EPS around the bacteria: (a) TEM image of the *A. caldus* morphology with no cadmium addition. (b) -(f) TEM images of *A. caldus* with cadmium addition and resulting CdS QDs biosynthesis. The CdS nanoparticles are disturbed around the bacteria (b), and selected-area electron diffraction (c) demonstrates that these nanoparticles are indeed CdS. A number of CdS QDs can be found in the extracellular polysaccharides (EPS) around the bacteria (d-f).

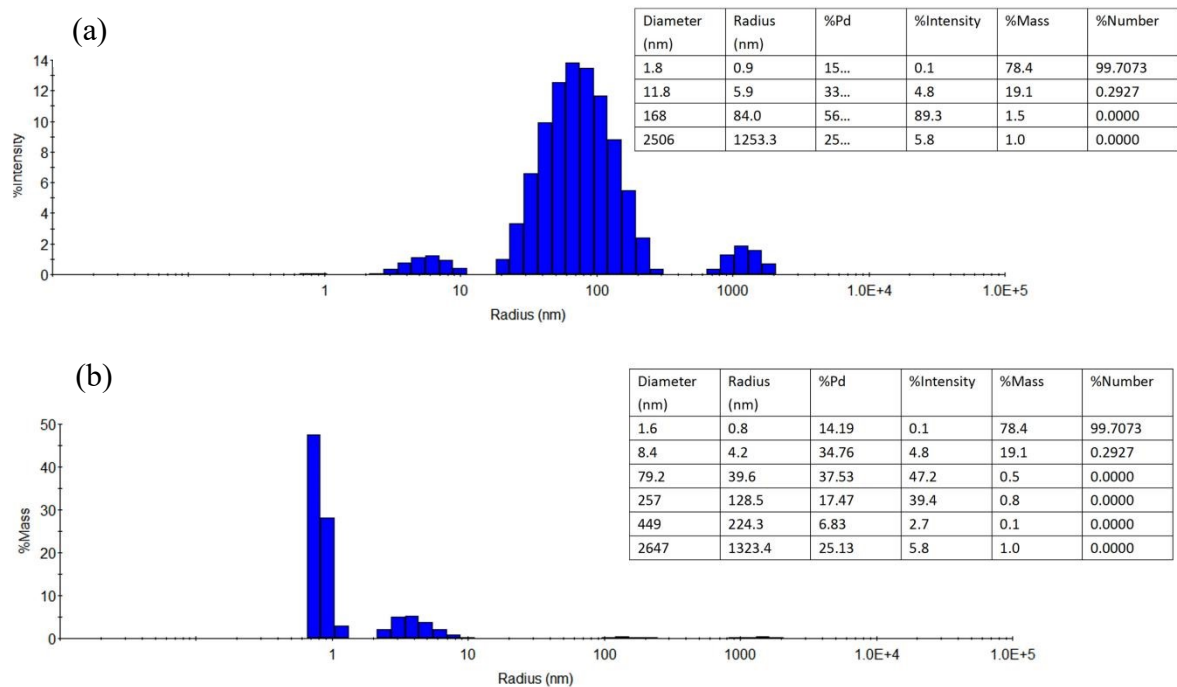
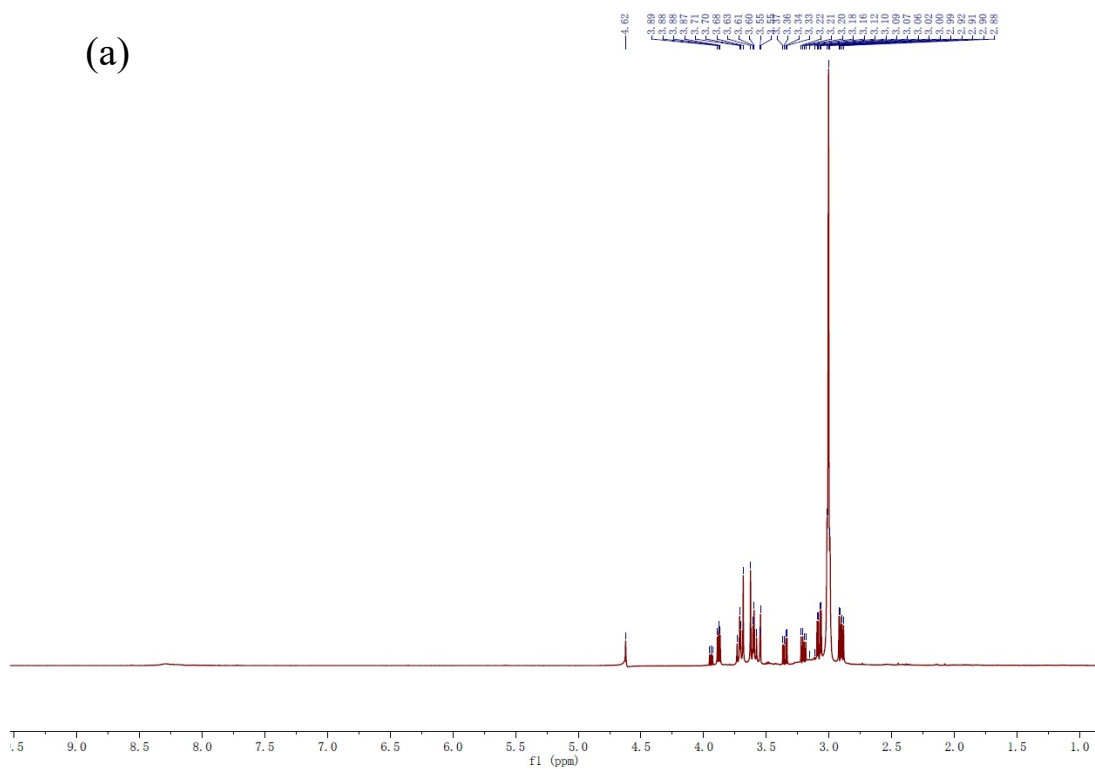
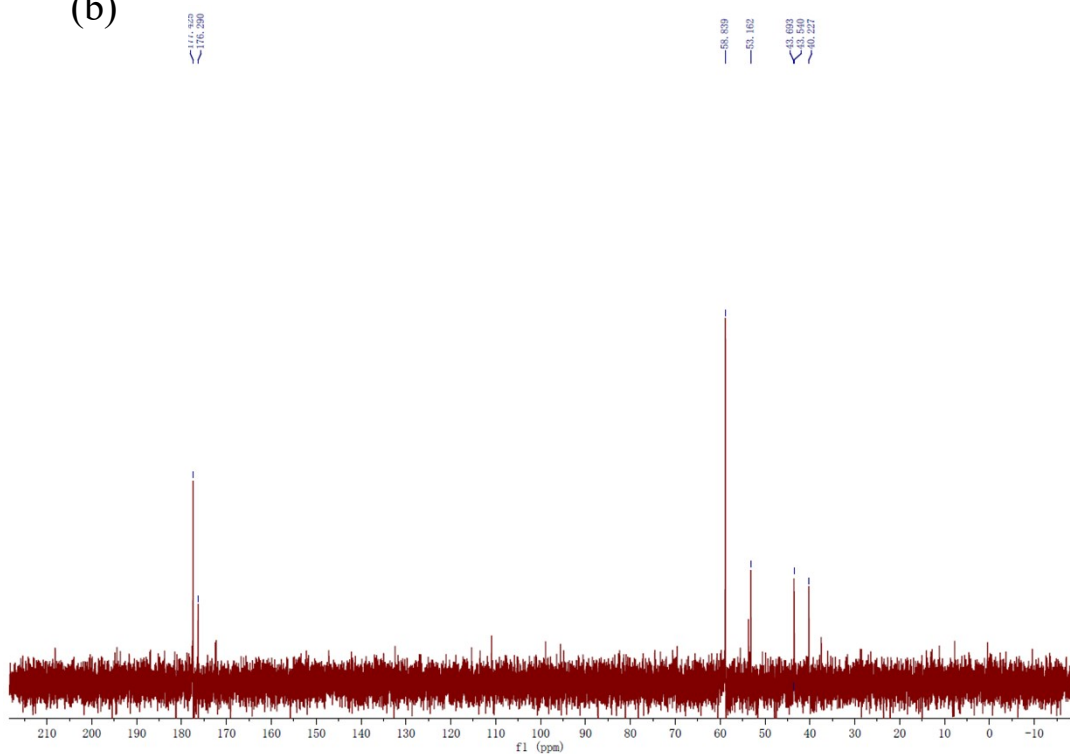


Figure S19. The hydrodynamic diameter of the CdS QDs transformed from cadmium electroplating waste by *Acidithiobacillus* sp., which is measured by dynamic light scattering. The result is displayed in (a) Intensity and (b) Mass, respectively.

(a)



(b)



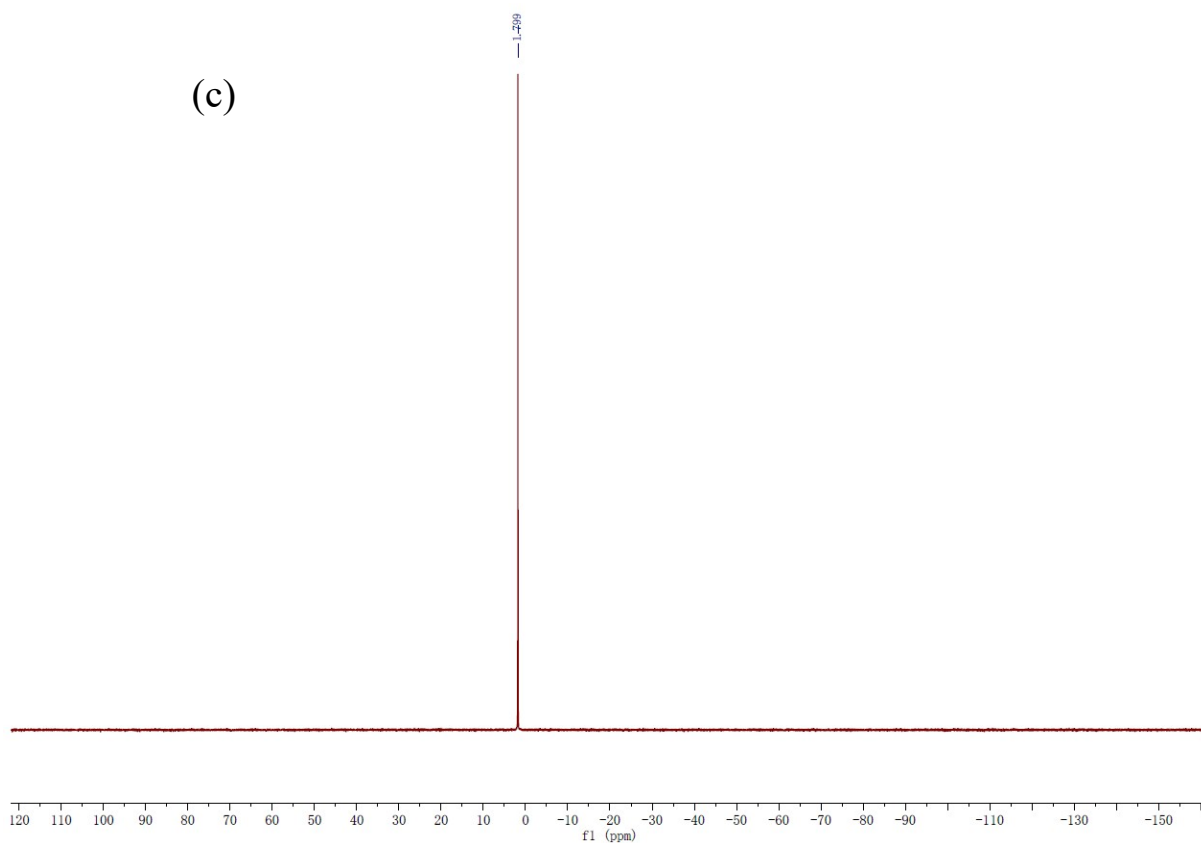


Figure S20. NMR data of the CdS QDs transformed from cadmium electroplating waste by *Acidithiobacillus* sp.: (a) ^1H , (b) ^{13}C , and (c) ^{31}P . These results imply that CdS QDs must contain many surface organic functional groups.

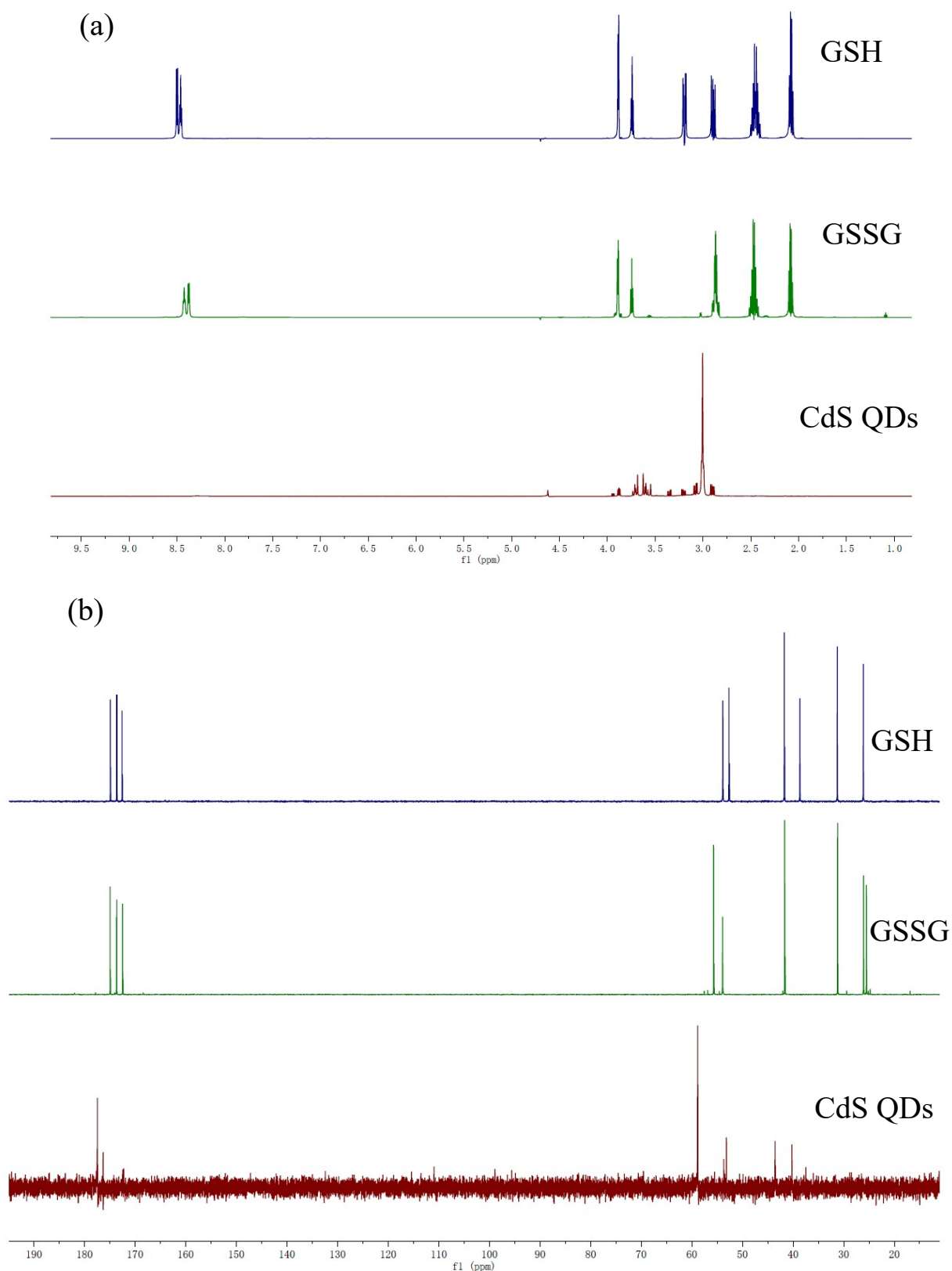


Figure S21. NMR data of the CdS QDs transformed from cadmium electroplating waste by *Acidithiobacillus* sp.: (a) ^1H spectra and (b) ^{13}C spectra of the comparison about GSH, GSSG and CdS QDs. These results imply that the surface organic functional groups on the CdS QDs are not GSH or GSSG.

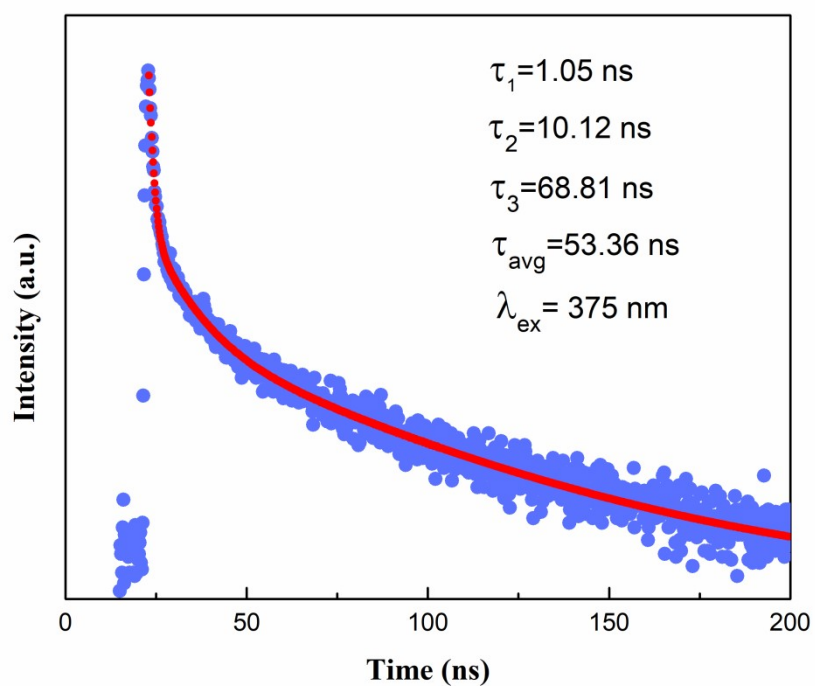


Figure S22. Time-resolved PL decay profile (using 375 nm excitation) of the CdS QDs after a long time placement, indicating that the fluorescence lifetime of CdS QDs transformed from cadmium electroplating waste by *Acidithiobacillus* sp. would also significantly decrease as the aggregation and growth of QDs over time in solution.

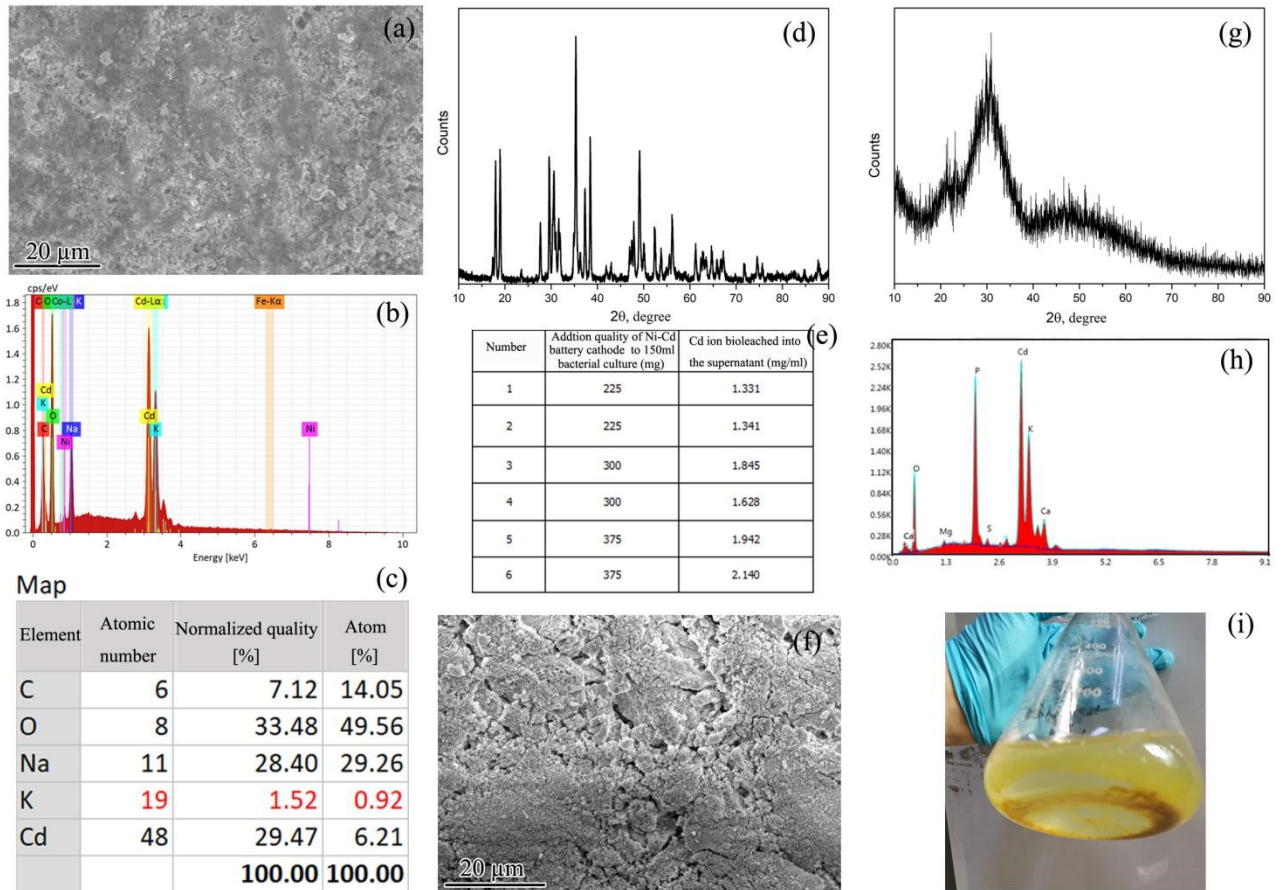


Figure S23. The waste Ni-Cd battery cathode was treated by using *Acidithiobacillus* sp. First, the Ni-Cd battery cathode was characterized by (a) SEM, (b) and (c) elemental information, and (d) XRD. Then, the Cd metal in the cathode is bioleached during the culture of *Acidithiobacillus* sp. (e) Relationships of the bioleaching of Cd^{2+} ions with different additions. After bioleaching, the bacterial solution was adjusted from acidic to neutral for CdS QD synthesis; in this process, large quantities of precipitated CdOH formed. (f) XRD pattern, (g) SEM image, (h) elemental information of the CdOH precipitation.

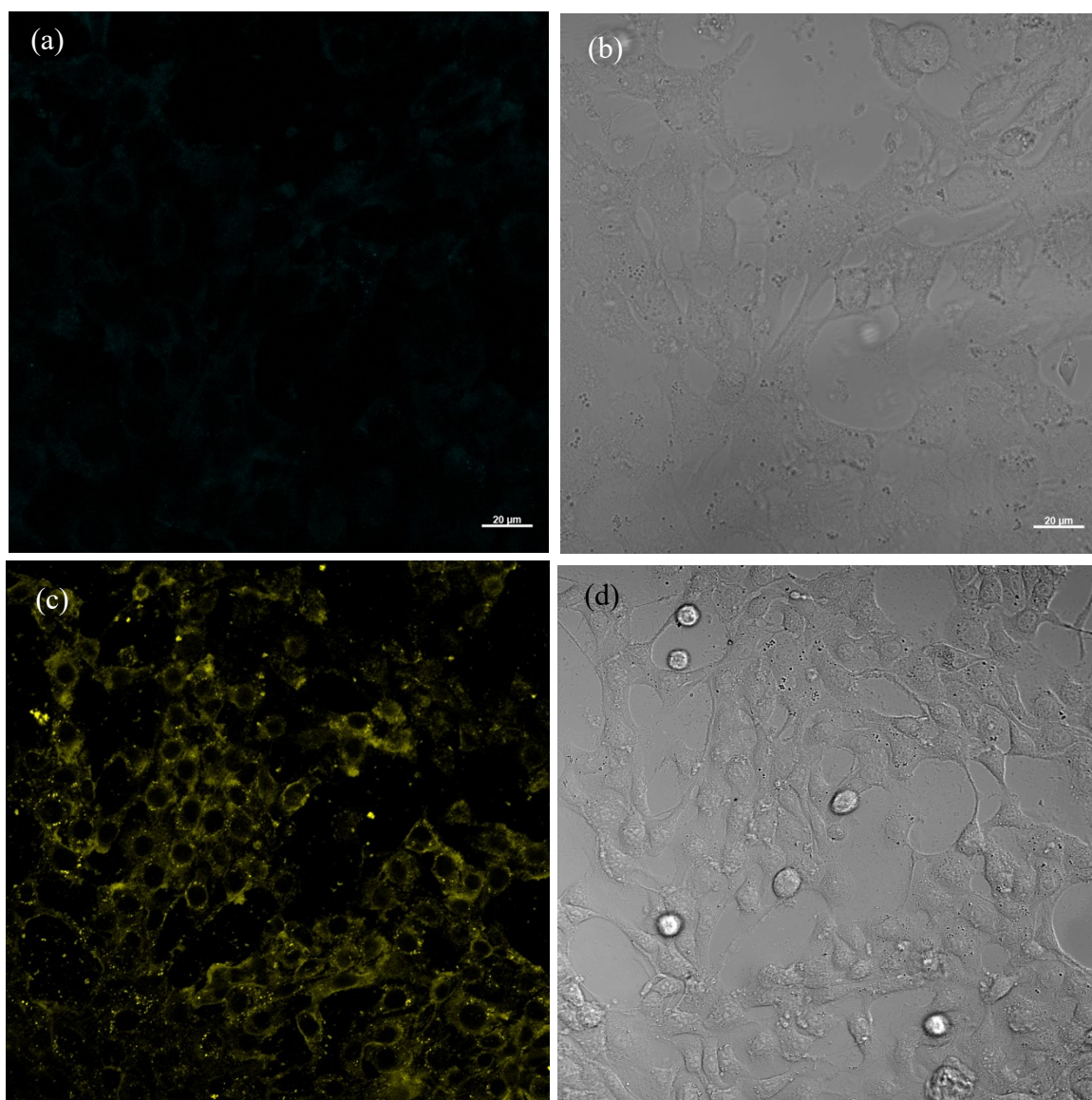


Figure S24. The bioimaging prospects of CdS QDs transformed from cadmium electroplating waste by *Acidithiobacillus* sp. were assessed. Fluorescence images were taken using a confocal laser scanning microscope at an excitation wavelength of 405 nm (a, c) and corresponding bright field images (b, d) of 4T1 mammary carcinoma cells after incubation without (a, b) or with (c, d) CdS quantum dots for 30 min.

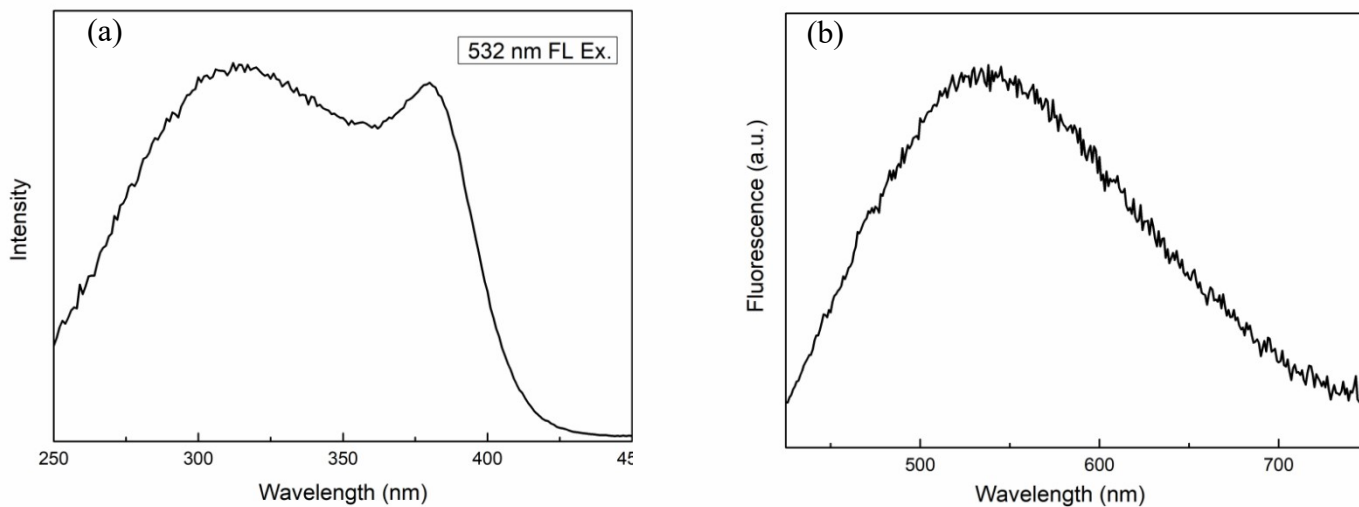


Figure S25. The fluorescence information of CdS QDs transformed from cadmium electroplating waste by *Acidithiobacillus* sp. (a) The excitation spectrum keeping the fluorescence emission wavelength at 532 nm. (b) Fluorescence spectra obtained using an excitation wavelength of 405 nm. These results suggest that using a confocal laser scanning microscope at an excitation wavelength of 405 nm, as shown in Figure S24, is appropriate.